

Quantification of edema reduction using differential quantitative T2 (DQT2) relaxometry mapping in recurrent glioblastoma treated with bevacizumab

Benjamin M. Ellingson · Timothy F. Cloughesy · Albert Lai ·
Phioanh L. Nghiemphu · Shadi Lalezari · Taryar Zaw ·
Kourosh Motevalibashinaeini · Paul S. Mischel · Whitney B. Pope

Received: 20 December 2010 / Accepted: 17 June 2011
© Springer Science+Business Media, LLC. 2011

Abstract The purpose of the current study was to quantify the reduction in T2 signal abnormality accompanying administration of the anti-angiogenic drug bevacizumab in recurrent glioblastoma (GBM) patients using a voxel-wise differential quantitative T2 (DQT2) mapping technique. Twenty-six patients with recurrent GBM treated with bevacizumab were scanned before and 4–6 weeks after treatment on a 1.5T clinical MR scanner. Quantitative T2 maps were created from proton density and T2-weighted images acquired using a standard multi-echo fast-spin echo sequence. T2 maps after treatment were co-registered with T2 maps prior to treatment in the same patient, and then voxel-wise subtraction was performed to create DQT2 maps for each patient. Results suggest DQT2 maps allow visualization and quantification of voxel-wise T2 changes resulting

from anti-VEGF therapy. Results demonstrated a significant decrease in T2 within pre-treatment T2 abnormal regions (mean reduction = 49.4 ms at 1.5T) following anti-VEGF treatment (Wilcoxon signed rank test, $P < 0.0001$). An elevated residual, post-treatment, median T2 was predictive of both progression-free (Log-rank, $P = 0.0074$) and overall survival (Log-rank, $P = 0.0393$).

Keywords GBM · Glioblastoma · Angiogenesis · DQT2 · Magnetic resonance imaging · MRI · Bevacizumab

Introduction

Glioblastoma multiforme (GBM) is the most common and most aggressive type primary brain tumor. Vascular endothelial growth factor (VEGF), a potent mediator of cerebrovascular permeability, and its receptors are often overexpressed in GBM compared to other types of brain tumors [1]. This overexpression of VEGF is thought to play a role in malignant transformation, tumor progression, and tumor angiogenesis [2, 3]. Thus, there has been considerable interest in therapeutics that target VEGF and its receptors for the treatment of recurrent GBM in order to reduce tumor angiogenesis and potentially slow tumor growth.

Bevacizumab, a monoclonal antibody to VEGF [4], has shown a progression-free survival (PFS) benefit [5–7] compared to historic controls [8]. These results, however, were based on a modified Macdonald criteria [9] that focuses primarily on the amount of contrast enhancement in T1-weighted images. Since anti-VEGF therapies significantly reduce the amount of contrast agent extravasation due to a decrease in vascular permeability [10, 11], the response assessment in neuro-oncology (RANO) criterion

B. M. Ellingson (✉) · T. Zaw · K. Motevalibashinaeini ·
W. B. Pope
Department of Radiological Sciences, David Geffen School
of Medicine, University of California Los Angeles, 924
Westwood Blvd., Suite 650, Los Angeles, CA 90095, USA
e-mail: bellingson@mednet.ucla.edu

B. M. Ellingson
Department of Biomedical Physics, David Geffen School
of Medicine, University of California Los Angeles,
Los Angeles, CA, USA

T. F. Cloughesy · A. Lai · P. L. Nghiemphu · S. Lalezari
Department of Neurology, David Geffen School of Medicine,
University of California Los Angeles, Los Angeles, CA, USA

P. S. Mischel
Department of Pathology and Laboratory Medicine,
David Geffen School of Medicine, University of California Los
Angeles, Los Angeles, CA, USA

was developed [12], which also takes into consideration the amount of non-enhancing tumor burden.

Although the T2-weighted signal abnormality is now used to assess changes in non-enhancing tumor burden and the extent of vasogenic edema according to the RANO criteria [12] and many studies have illustrated the dramatic reduction in vasogenic edema after administration of anti-VEGF therapy as measured on T2-weighted images [5, 10, 11, 13], no studies have actually quantified the change in T2 associated with administration of anti-VEGF therapies. In the current study, we quantify the distribution of T2 before and after treatment with anti-VEGF therapy within regions of containing both suspected non-enhancing tumor and vasogenic edema, explore the voxel-wise change in T2 due to anti-VEGF therapy using a novel technique termed differential quantitative T2 (DQT2) mapping, and determine if these parameters are predictive of PFS and overall survival (OS) in recurrent GBM treated with bevacizumab.

Materials and methods

Patients

All patients participating in this study signed institutional review board-approved informed consent to have their data in our institution's neuro-oncology database. Data acquisition was performed in compliance with all applicable Health Insurance Portability and Accountability Act (HIPAA) regulations. The study spanned 11-15-2005 to 8-31-2010. Patients were retrospectively selected from our institution's neuro-oncology database. A total of $n = 26$ patients who met the following criteria were selected: (1) pathology confirmed GBM with recurrence based on MRI and clinical data, (2) regularly treated every 2 weeks per cycle with bevacizumab (Avastin, Genentech, South San Francisco, CA; 5 or 10 mg/kg body weight), alone ($n = 1$), or in combination with chemotherapy (carboplatin, $n = 3$; irinotecan, $n = 20$; lomustine, $n = 2$), and (3) baseline (pre-bevacizumab treatment) and minimum of one follow-up MRI scans that include multiple echo T2 images (proton density + T2-weighted images) before and after treatment. In the rest of the patients treated with bevacizumab between 2005 and 2010, fluid attenuated inversion recovery (FLAIR) images were used instead of multiecho T2 images. Baseline scans were obtained approximately 1 week pre-treatment (mean = 6.9 days \pm 2.5 days SEM). Follow-up scans were obtained at approximately 4–6 week intervals (mean = 32 days \pm 3.0 days SEM). At the time of last assessment (August, 2010) all patients but one had progressed and all patients but one were deceased. For bevacizumab-treated patients, 16 patients were on steroids at the time of initial imaging

(dose range 0.75–48 mg dexamethasone) and 10 patients were not on steroids. Of the 16 patients on steroids, 6 patients had no change in dose between the MRI scans examined, 3 patients had a decrease in steroid dose, and 7 patients had an increase in steroid dose. A total of 10 patients were treated at first recurrence, 9 at second recurrence, and 7 at third or more recurrence. Karnofsky Performance Score (KPS) ranged from 40 to 90 and averaged around 80. Approximately 19% (5/26) of patients had a decline in KPS between MRI scans, one patient improved, and the rest had no change. All patients were treated with radiation therapy (typically 6000 cGy) and maximal tumor resection at time of initial tumor presentation.

Magnetic resonance imaging

Data was collected on a 1.5T MR system (General Electric Medical Systems, Waukesha, WI) using pulse sequences supplied by the scanner manufacturer. Standard anatomical MRI sequences included axial T1 weighted (TE/TR = 15 ms/400 ms, slice thickness = 5 mm with 1 mm interslice distance, number of excitations (NEX) = 2, matrix size = 256 \times 256, and field-of-view (FOV) = 24 cm), proton density weighted images (TE/TR = 9.6–16 ms/4000 ms, slice thickness = 5 mm with 1 mm interslice distance, NEX = 2, matrix size = 256 \times 256, and FOV = 24 cm), T2 weighted fast spin-echo (TE/TR = 126–130 ms/4000 ms, slice thickness = 5 mm with 1 mm interslice distance, NEX = 2, matrix size = 256 \times 256, and FOV = 24 cm), and FLAIR images (TI = 2200 ms, TE/TR = 120 ms/4000 ms, slice thickness = 5 mm with 1 mm interslice distance, NEX = 2, matrix size = 256 \times 256, and FOV = 24 cm). Additionally, gadopentetate dimeglumine enhanced (Magnevist; Berlex, Wayne, NJ; 0.1 mmol/kg) axial and coronal T1 weighted images (coronal: TE/TR = 15 ms/400 ms, slice thickness 3 mm with 1 mm interslice distance, NEX = 2, a matrix size of 256 \times 256, and FOV = 24 cm) were acquired immediately after contrast injection. Quantitative T2 maps were generated using the effective echo times from the two echoes acquired during a fast-spin echo preparation (i.e., using the proton density and T2-weighted images).

Definition of disease progression

Disease progression was defined by both the standard Macdonald criteria [9], indicated by a 25% increase in enhancing tumor, as well as a modified criteria that includes progression of a non-enhancing tumor evident by an increased mass effect and/or architectural distortion such as blurring of the gray–white interface [14]. Both progression-free survival (PFS) and overall survival (OS) were with respect to the post-treatment MRI scan date.

Differential quantitative T2 (DQT2) mapping

All images for each patient were registered to a high-resolution (1.0 mm isotropic), T1-weighted brain atlas (MNI152; Montreal Neurological Institute) using a mutual information algorithm and a 12-degree of freedom transformation using FSL (FMRIB, Oxford, UK; <http://www.fmrib.ox.ac.uk/fsl/>). Fine registration (1–2 degrees and 1–2 voxels) was then performed using a Fourier transform-based, 6-degree of freedom, rigid body registration algorithm [15] followed by visual inspection to ensure adequate alignment. After proper registration was visually verified, voxel-wise subtraction was performed between T2 maps acquired post-treatment and baseline, pre-treatment T2 maps to create the resulting DQT2 maps.

Region of interest (ROI) determination

In the current study, we chose to examine T2 distributions in regions of T2 ($n = 24$) or FLAIR signal abnormality ($n = 2$) on pre-treatment T2-weighted or FLAIR images. No cases were mixed T2 and FLAIR ROIs. FLAIR and T2-weighted images were acquired pre-contrast. This ROI was chosen based on RANO recommendations, the observation that tumor infiltration into normal brain parenchyma typically results in an increase in T2-weighted, or FLAIR, abnormal signal [16–19], and recommendations from multiple investigations suggesting that T2 signal abnormalities should be routinely used to visualize the extent of malignant infiltrating tumor [20–24]. ROIs were created using a semi-automated, thresholding and region-growing technique described in a previous publication [25]. In order to assess reproducibility of the T2 measurements we also measured T2 within a 5 mm diameter spherical ROI placed within normal-appearing white matter near the cingulate cortex (i.e., cingulum bundle) both pre- and post-treatment.

Hypothesis testing

Based on results from previous investigations [5, 10, 11, 13], we hypothesized that administration of anti-VEGF therapeutics would result in a significant reduction of vasogenic edema leading to a decrease in measured T2. In order to test this hypothesis, we performed a non-parametric, paired Wilcoxon signed rank test on the median T2 within the regions of pre-treatment abnormal T2 signal, evaluated both pre- and post-treatment.

Next, we explored whether the median T2 within regions of pre-treatment abnormal T2 signal evaluated pre- and post-treatment were significant predictors of PFS or OS, which are common clinical endpoints. We also explored whether the median *difference in T2*, as measured with DQT2 mapping, was a significant predictor of PFS or

OS. Survival analysis was performed using linear regression and log-rank statistical analysis on Kaplan–Meier data. All statistical tests were performed using GraphPad Prism[®] version 4.0.

Results

Approximately 88% (23 of 26) of patients examined had either a reduction in contrast enhancement or a reduction in T2/FLAIR signal abnormality at the first follow-up time after administration of bevacizumab. Approximately 77% (20 of 26) had both a decrease in contrast enhancement and reduction in T2/FLAIR signal abnormality. The mean PFS was 167.5 ± 34.5 days SEM (median PFS = 114.5 days) and the mean OS was 300.2 ± 49.1 days SEM (median OS = 248 days) for all patients evaluated from the time of the post-treatment MRI scans.

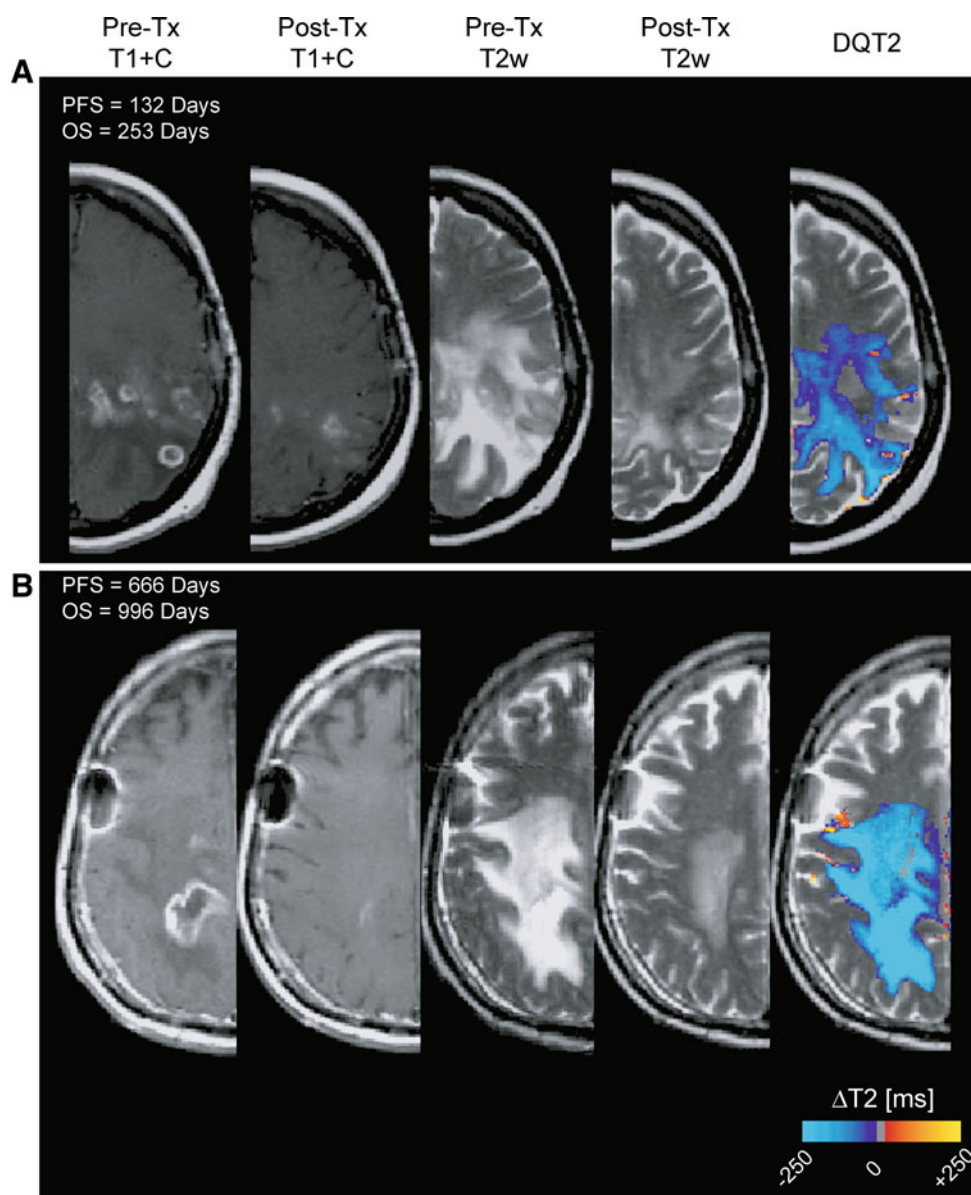
DQT2 maps allow visualization and quantification of voxel-wise T2 changes

For the majority of patients, standard post-contrast T1-weighted and T2-weighted images demonstrated significant changes following the first dose of bevacizumab (Fig. 1). This change in T2-weighted image features was also evident on quantitative T2 maps and easily visualized and quantified using the DQT2 mapping technique. Specifically, qualitative examination of DQT2 maps suggested patients having a larger decrease in T2 following the first treatment of bevacizumab were more likely to have a longer PFS and OS. Figure 1a illustrates standard MR images before and after treatment in a patient with a modest PFS and OS. Note that the DQT2 images showed a subtle decrease in T2 within areas of signal abnormality on pre-treatment T2-weighted images. On the other hand, Fig. 1b demonstrated a patient with a similar radiographic response on standard MR images; however, DQT2 images showed a substantial reduction in T2 within areas of pre-treatment T2 signal abnormality. These results suggest DQT2 maps may provide added value to standard anatomical MR evaluation of response to bevacizumab.

Anti-VEGF therapy results in a significant reduction in tissue T2

As expected, the distribution of T2 within regions of abnormal T2 signal intensity prior to treatment were significantly elevated with respect to normal white matter for all patients (Fig. 2a; *F-test, mean T2 vs. 77.4 ms from [26], $P < 0.0001$ for all patients*). Similarly, the distribution of T2 within pre-treatment regions of abnormal T2 signal intensity evaluated after treatment were also elevated with

Fig. 1 Effects of anti-VEGF therapy on post-contrast T1-weighted images and pre-contrast T2-weighted images on conventional MRI and differential quantitative T2 (DQT2) maps. **a** Patient with a relatively short progression-free survival (PFS) and overall survival (OS) despite a radiographic response on standard MR images. DQT2 maps demonstrate only a moderate reduction in T2 within non-enhancing tumor regions. **b** Patient with a long PFS and OS showing a similar radiographic response on standard MR images to patient in **a**; however, DQT2 maps show a significantly larger decrease in T2 within regions suspected of containing non-enhancing tumor or edema



respect to normal white matter (Fig. 2b; *F-test, mean T2 vs. 77.4 ms from [26], $P < 0.0001$ for all patients*).

Results suggest anti-VEGF therapy leads to a significant reduction of tissue T2 within regions of long T2, while maintaining T2 within regions of normal pre-treatment T2. Median T2 within pre-treatment T2/FLAIR signal abnormality was significantly reduced after treatment compared to the median T2 estimate prior to treatment (Fig. 2d; *Wilcoxon signed rank test, pre- vs. post-treatment, $P < 0.0001$*). Similarly, DQT2 maps generated after administration of bevacizumab suggest a significant reduction in T2 (Fig. 2c; *F-test, mean $\Delta T2$ vs. 0 ms, $P < 0.0001$ for all patients*). Note that for the first comparison we used the median T2 pre- and post-treatment to examine the

magnitude of the effect, whereas for the second comparison (i.e., using DQT2 mapping) we examined the median voxel-wise change in T2. These two techniques provided statistically distinct estimates of the reduction in T2 after bevacizumab (*Wilcoxon signed rank test, median T2 pre-treatment—median T2 post-treatment vs. median $\Delta T2$ from voxel-wise DQT2 mapping, $P = 0.002$*). In regions of normal appearing white matter within the cingulate cortex (i.e., cingulum), tissue T2 measured approximately 101 ms and there was no change after treatment (Fig. 2e; *Wilcoxon signed rank test, pre- vs. post-treatment, $P = 0.9268$*). These results support the hypothesis that anti-VEGF therapy reduces vasogenic edema, which is manifested as a decrease in tissue T2 on MRI, and the DQT2 mapping

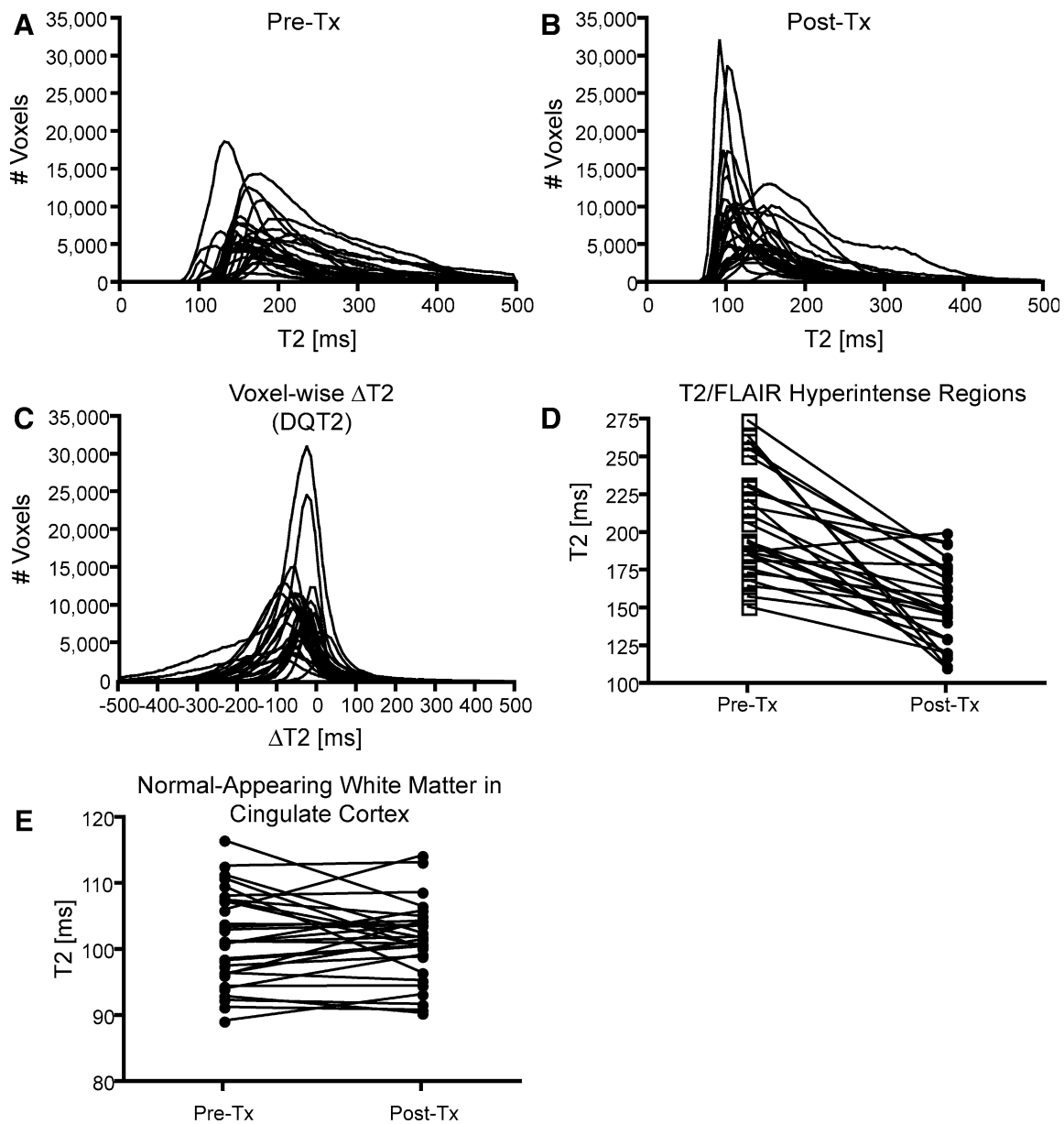


Fig. 2 Distribution of T2 within regions of suspected tumor and/or edema **a** before and **b** after administration of anti-VEGF therapy. **c** Distributions of $\Delta T2$ from DQT2 mapping shows an overall reduction in T2 within these areas. **d** Median T2 pre- and post-treatment showing an overall reduction in T2 after treatment with

anti-VEGF therapy (Wilcoxon Rank Sum, $P < 0.0001$). **e** Pre- and post-treatment T2 measurements in normal appearing white matter within the cingulate cortex showing no change in T2 in normal tissue after anti-VEGF therapy (Wilcoxon Rank Sum, $P = 0.9268$)

technique provides a unique perspective on the change in T2 accompanying anti-VEGF therapy.

Median post-treatment T2 predicts progression-free and overall survival

Regression results suggest the median post-treatment T2 was linearly correlated with both PFS (Fig. 3a; *Pearson's correlation coefficient*, $R^2 = 0.1711$, $P = 0.0398$) and OS (Fig. 3b; $R^2 = 0.1947$, $P = 0.0272$); however, no linear

trend was found between median pre-treatment T2 and either PFS (Fig. 3a; *Pearson's correlation coefficient*, $R^2 = 0.0127$, $P = 0.5918$) or OS (Fig. 3b; $R^2 = 0.0483$, $P = 0.2913$). In particular, patients having a lower median T2 post-treatment were more likely to progress later and live longer than patients having a higher median T2 after the first treatment. DQT2 estimates of median $\Delta T2$ were significantly correlated with OS (Fig. 3d; *Pearson's correlation coefficient*, $R^2 = 0.2267$, $P = 0.0161$), but not PFS (Fig. 3c; $R^2 = 0.1190$, $P = 0.0912$). Although the

correlation coefficient was relatively low for all parameters examined, results suggest patients showing a low T2 after bevacizumab, or larger change in T2 as a result of bevacizumab treatment, may be more likely to progress later and live longer than patients having a higher post-treatment T2 or lower magnitude of change in T2.

Log-rank analysis of Kaplan–Meier survival data suggested that patients having a post-treatment median T2 higher than 160 ms were more likely to progress earlier than patients having a post-treatment median T2 lower than 160 ms (Fig. 4a; PFS: *Log-rank*, $P = 0.0074$) as well as have a shorter overall survival (Fig. 4b; OS: *Log-rank*, $P = 0.0393$). Interestingly, results suggested no progression-free or overall survival advantage for those having a median reduction in T2, as measured with DQT2 maps, higher or lower than 25 ms (Fig. 4b, c; PFS: *Log-rank*, $P = 0.2203$; OS: *Log-rank*, $P = 0.3761$). These results suggest post-treatment median T2 may be a valuable predictive imaging biomarker for early disease progression and overall survival in recurrent GBM treated with bevacizumab.

Discussion

Although most studies examining the effects of anti-VEGF therapy have noted a reduction in vascular permeability

resulting in decreased vasogenic edema as manifested on T2-weighted images [27–30], this is the first study to find that treatment with anti-VEGF therapy results in a significant reduction in tissue T2 within regions of T2/FLAIR signal abnormality thought to contain both non-enhancing tumor and vasogenic edema. Specifically, we found a decrease in tissue T2 around 50 ms (at a field strength of 1.5T) with respect to pre-treatment T2/FLAIR abnormal regions, which is likely due to the reduction in water concentration within these brain regions.

Another important finding in the current study worth noting is that DQT2 maps provide additional insight into regional changes in T2 as a result of anti-VEGF treatment beyond that of conventional MR imaging or simple comparison of pre- and post-treatment T2 maps. Previous investigations examining the volumetric changes in tissue having T2 hyperintensity found no correlation with the degree of volume change and patient survival [25]. As demonstrated in Fig. 1, the volume extent of tissue having abnormal T2 hyperintensity is independent of the degree of change in tissue T2, largely due to the extreme heterogeneity of human GBM. The use of voxel-wise changes in MR parameters, however, is not a completely novel concept. Voxel-wise changes in apparent diffusion coefficients from diffusion MRI [31–33] and relative cerebral blood volume from perfusion MRI [34] have been proposed as

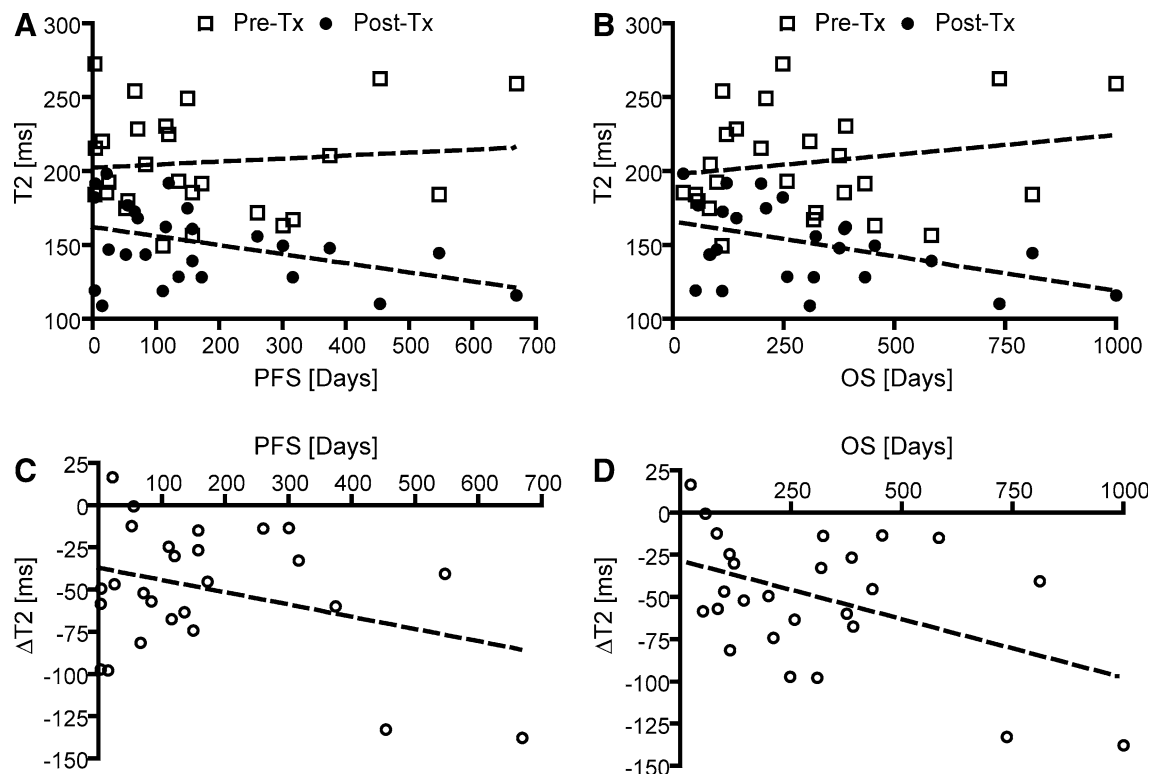


Fig. 3 Scatter plots showing trends between **a, b** pre- and post-treatment median T2 and **c, d** $\Delta T2$ from DQT2 mapping as a function of progression-free survival (PFS) or overall survival (OS)

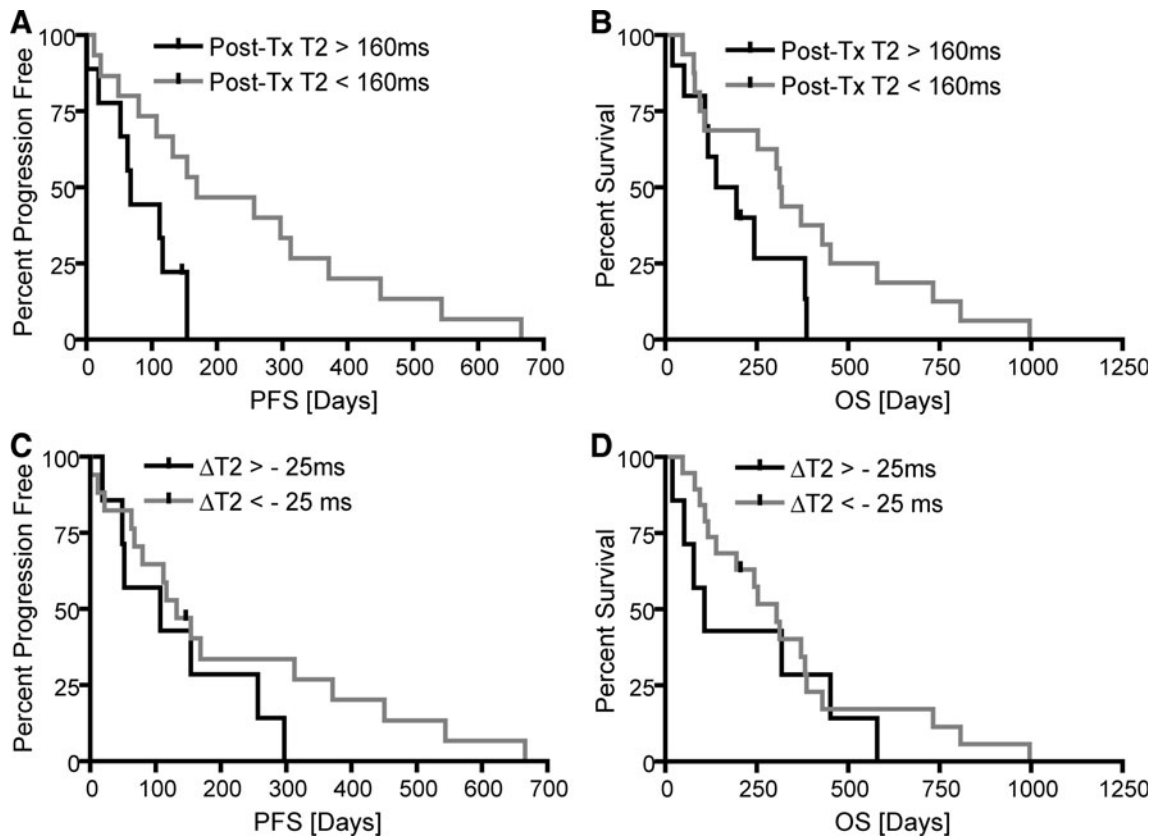


Fig. 4 Kaplan–Meier curves for progression-free (PFS) and overall survival (OS) stratifying patients by **a, b** post-treatment (Tx) median T2 higher or lower than 160 ms, or **c, d** median Δ T2 for DQT2 higher or lower than a 25 ms reduction (note lower than 25 ms reduction is considered *more* reduction). The median PFS for patients having a post-treatment median T2 higher than 160 ms was 68 days, compared

with a median PFS of 169 days for patients having a post-treatment median T2 lower than 160 ms. Median OS for patients having a post-treatment median T2 higher than 160 ms was 166.5 days, compared with a median OS of 315.5 days for patients having a post-treatment median T2 lower than 160 ms

useful imaging biomarkers for the evaluation of human gliomas. Additionally, voxel-wise changes in T2 have been utilized to characterize neurodegenerative changes, including multiple sclerosis [35]; however, these voxel-wise analyses are typically performed across patients instead of within the same patient over time. As such, this is the first study to demonstrate the possible utility of voxel-wise changes in T2, termed DQT2 mapping, as a method for evaluating changes in edematous tissue over time.

Similar to other imaging studies involving anti-VEGF therapy, our results suggest early T2 *changes* did not seem to be particularly useful in predicting patient outcomes after treatment; however, our results have demonstrated that median post-treatment T2 was able to significantly stratify short and long-term PFS and OS. The lack of robust prediction of clinical endpoints using the *change* in T2 suggests that a change in water concentration due to clearing of vasogenic edema ultimately does not reflect the inherent aggressiveness of the tumor, nor does it reflect growth characteristics, which are both thought to influence

overall patient survival in GBM. Interestingly, our results demonstrate that an elevated residual, or post-treatment, T2 is a significant predictor of both PFS and OS. In combination with a recent study demonstrating that residual contrast-enhancement also predicts PFS and OS [25], our results suggest that the amount of abnormal signal *after* the first treatment with bevacizumab is predictive of long-term progression-free and overall survival.

It is important to mention that many valuable biomarkers have shown the ability to predict patient survival in anti-angiogenic therapies, including [18 F]-fluorothymidine PET [36], dynamic contrast-enhanced (DCE)-MRI combined with blood serum markers [37], pre-treatment diffusion MR characteristics [38], conventional MR imaging characteristics [25], and functional diffusion maps (fDMs) using serial diffusion MR data [39, 40]. These techniques, however, are distinctly different from the DQT2 mapping technique in that they quantify particular aspects of tumor growth, metabolism, or vasculature instead of changes in tissue T2 characteristics likely due to change in water homeostasis.

Technical limitations and considerations

One possible limitation to the current manuscript is the use of only two echo times to estimate T2 characteristics for the tissue. It is possible that the variability in T2 measurements within the regions of interest may have been significantly lower if more echoes were collected; however, due to the retrospective nature of the current study we were only able to estimate T2 from two echoes. To address questions on reproducibility, T2 measurements were taken from regions of normal-appearing white matter within the cingulate cortex. The average value of tissue T2 pre-treatment was found to be 101.8 ± 1.3 ms (standard error of the mean) and post-treatment was estimated at 101.3 ± 1.1 ms, which is consistent with previous multiecho estimates of normal white matter from the literature [41]. These results suggest T2 measurements from only two echoes in the current study likely do not vary considerably from T2 measurements acquired using more echoes.

Contributions of changes in steroid dose and concomitant chemotherapy on tissue T2 were also a possible limitation in the current study. Corticosteroids are known to reduce vasogenic edema in GBMs, which is manifested as a reduction in T2 hyperintensity. Increasing steroid doses were present in 7 of the 26 patients in the current study. Additionally, changes in tissue T2 may have resulted from concomitant chemotherapy, which occurred in 25 of the 26 patients in the current study. Future studies examining changes in T2 resulting from bevacizumab monotherapy are necessary to determine the precise contributions of each of these factors.

An additional limitation to the current technique is the use of a rigid-body image transformation in order to register T2 maps to the baseline images. Significant mass effect from tumor growth or intracranial pressure induced by edema may cause inaccuracies in the registration between T2 maps and anatomical datasets. Suspected tumor regions near gyri, sulci, or the ventricles should be considered with caution, since erroneous results in these regions can occur as a result of misregistration. To overcome these challenges, we chose to use two sequential automated registration steps followed by manual inspection. In addition, we attempted to exclude regions suspected of containing cerebrospinal fluid contamination from image misregistration near boundaries of tissue mismatch. An additional step of elastic (non-linear) registration may potentially be beneficial for the registration of significantly distorted datasets. The last limitation to the current study was the size of our patient population. Although our database contains over 300 patients with recurrent GBM treated with anti-VEGF therapies, only 26 had pre- and post-treatment proton density and T2-weighted images that could be used for calculation of T2 maps. It

is conceivable that a larger patient cohort may be beneficial to more definitively determine whether DQT2 mapping is a valuable surrogate biomarker for patient survival.

In summary, the current results suggest that DQT2 mapping may be advantageous for evaluating changes in tissue water content (i.e., edema) such as the expected changes following anti-angiogenic therapy.

Acknowledgment This study was supported by grants from Brain Tumor Funders Collaborative (WBP); Art of the Brain (TFC); Ziering Family Foundation in memory of Sigi Ziering (TFC); Singleton Family Foundation (TFC); and Clarence Klein Fund for Neuro-Oncology (TFC).

References

- Huang H, Held-Feindt J, Buhl R, Mehdorn HM, Mentlein R (2005) Expression of VEGF and its receptors in different brain tumors. *Neurol Res* 27(4):371–377
- Plate KH, Breier G, Risau W (1994) Molecular mechanisms of developmental and tumor angiogenesis. *Brain Pathol* 4(3): 207–218
- Holash J, Maisonpierre PC, Compton D, Boland P, Alexander CR, Zagzag D, Yancopoulos GD, Weigand SJ (1999) Vessel cooption, regression, and growth in tumors mediated by angiotensins and VEGF. *Science* 284(5422):1994–1998
- Duda DG, Batchelor TT, Willett CG, Jain RK (2007) VEGF-targeted cancer therapy strategies: current progress, hurdles and future prospects. *Trends Mol Med* 13(6):223–230
- Nghiempu PL, Liu W, Lee Y, Than T, Graham C, Lai A, Green RM, Pope WB, Liao LM, Mischel PS, Nelson SF, Elashoff R, Cloughesy TF (2009) Bevacizumab and chemotherapy for recurrent glioblastoma: a single-institution experience. *Neurology* 72(14):1217–1222
- Vredenburgh JJ, Desjardins A, Herndon JE, Dowell JM, Reardon DA, Quinn JA, Rich JN, Sathornsumetee S, Gururangan S, Wagner M, Bigner DD, Friedman AH, Friedman HS (2007) Phase II trial of bevacizumab and irinotecan in recurrent malignant glioma. *Clin Cancer Res* 13:1253–1259
- Friedman AH, Prados MD, Wen PY, Mikkelsen T, Schiff D, Abrey LE, Yung WK, Paleologos N, Nicholas MK, Jensen R, Vredenburgh J, Huang J, Zheng M, Cloughesy T (2009) Bevacizumab alone and in combination with irinotecan in recurrent glioblastoma. *J Clin Oncol* 27(28):4733–4740
- Stupp R, Mason WP, van den Bent MJ, Weller M, Fisher B, Taphoorn MJ, Belanger K, Brandes AA, Morosi C, Bogdahn U, Curschmann J, Janzer RC, Ludwin SK, Gorlia T, Allgeier A, Lacombe D, Cairncross JG, Eisenhauer E, Mirimanoff RO (2005) Radiotherapy plus concomitant and adjuvant temozolomide for glioblastoma. *N Engl J Med* 352(10):987–996
- Macdonald DR, Cascino TL, Schold SC Jr, Cairncross JG (1990) Response criteria for phase II studies of supratentorial malignant glioma. *J Clin Oncol* 8(7):1277–1280
- Iwamoto FM, Abrey LE, Beal K, Gutin PH, Rosenblum ML, Reuter VE, DeAngelis LM, Lassman AB (2009) Patterns of relapse and prognosis after bevacizumab failure in recurrent glioblastoma. *Neurology* 73(15):1200–1206
- Norden AD, Young GS, Setayesh K, Mizukansky A, Klufas R, Ross GL, Ciampa AS, Ebbeling LG, Levy B, Drappatz J, Kesari S, Wen PY (2008) Bevacizumab for recurrent malignant gliomas: efficacy, toxicity, and patterns of recurrence. *Neurology* 70(10): 779–787

12. Wen PY, Macdonald DR, Reardon DA, Cloughesy TF, Sorensen AG, Galanis E, de Groot JF, Wick W, Gilbert MR, Lassman AB, Tsien CI, Mikkelsen T, Wong ET, Chamberlain MC, Stupp R, Lamborn KR, Vogelbaum MA, van den Bent MJ, Chang SM (2010) Updated response assessment criteria for high-grade gliomas: response assessment in neuro-oncology working group. *J Clin Oncol* 28:1963–1972
13. Zuniga RM, Torcuator R, Jain R, Anderson J, Doyle T, Ellika S, Schultz L, Mikkelsen T (2009) Efficacy, safety and patterns of response and recurrence in patients with recurrent high-grade gliomas treated with bevacizumab plus irinotecan. *J Neurooncol* 91(3): 329–335
14. Pope WB, Sayre J, Perlina A, Villablanca JP, Mischel PS, Cloughesy TF (2005) MR imaging correlates of survival in patients with high-grade gliomas. *AJNR Am J Neuroradiol* 26(10):2466–2474
15. Cox RW, Jesmanowicz A (1999) Real-time 3D image registration for functional MRI. *Magn Reson Med* 42:1014–1018
16. Earnest F IV, Kelly PJ, Scheithauer BW, Kall BA, Cascino TL, Ehman RL, Forbes GS, Axley PL (1988) Cerebral astrocytomas: histopathologic correlation of MR and CT contrast enhancement with stereotactic biopsy. *Radiology* 166(3):823–827
17. Kelly PJ, Daumas-Duport C, Kispert DB, Kall BA, Scheithauer BW, Illig JJ (1987) Imaging-based stereotaxic serial biopsies in untreated intracranial glial neoplasms. *J Neurosurg* 66(6):865–874
18. Kelly PJ, Daumas-Duport C, Scheithauer BW, Kall BA, Kispert DB (1987) Stereotactic histological correlations of computed tomography- and magnetic resonance imaging-defined abnormalities in patients with glial neoplasms. *Mayo Clin Proc* 62(6): 450–459
19. Watanabe M, Tanaka R, Takeda N (1992) Magnetic resonance imaging and histopathology of cerebral gliomas. *Neuroradiology* 34(6):463–469
20. Brant-Zawadzki M, Norman D, Newton TH (1984) Magnetic resonance imaging of the brain: the optimal screening technique. *Radiology* 152:71–77
21. Byrne TN (1994) Imaging of gliomas. *Semin Oncol* 21:162–171
22. Husstedt HW, Sickert M, Köstler H, Haubitz B, Becker H (2000) Diagnostic value of the fast-FLAIR sequence in MR imaging of intracranial tumors. *Eur Radiol* 10(5):745–752
23. Tsuchiya K, Mizutani Y, Hachiya J (1996) Preliminary evaluation of fluid-attenuated inversion-recovery MR in the diagnosis of intracranial tumors. *AJNR Am J Neuroradiol* 17(6):1081–1086
24. Essig M, Hawighorst H, Schoenberg SO, Engenhart-Cabillie R, Fuss M, Debus J, Zuna I, Knopp MV, van Kaick G (1998) Fast fluid-attenuated inversion-recovery (FLAIR) MRI in the assessment of intraaxial brain tumors. *J Magn Reson Imaging* 8(4):789–798
25. Ellingson BM, Cloughesy TF, Lai A, Nghiemphu PL, Mischel PS, Pope WB (2011) Quantitative volumetric analysis of conventional magnetic resonance imaging response in recurrent glioblastoma treated with bevacizumab. *Neuro Oncol* 13:401–409
26. Whittall KP, Mackay AL, Graeb DA, Nugent RA, Li DKB, Paty DW (1997) In vivo measurement of T2 distributions and water contents in normal human brain. *Magn Reson Med* 37(1):34–43
27. Ananthnarayan S, Bahng J, Roring J, Nghiemphu P, Lai A, Cloughesy T, Pope WB (2008) Time course of imaging changes of GBM during extended bevacizumab treatment. *J Neurooncol* 88(3):339–347
28. Bokstein F, Shpigel S, Blumenthal DT (2008) Treatment with bevacizumab and irinotecan for recurrent high-grade glial tumors. *Cancer* 112(10):2267–2273
29. Fischer I, Cunliffe CH, Bollo RJ, Raza S, Monoky D, Chiriboga L, Parker EC, Golfinos JG, Kelly PJ, Knopp EA, Gruber ML, Zagzag D, Narayana A (2008) High-grade glioma before and after treatment with radiation and Avastin: initial observations. *Neuro Oncol* 10(5):700–708
30. Pope WB, Lai A, Nghiemphu P, Mischel P, Cloughesy TF (2006) MRI in patients with high-grade gliomas treated with bevacizumab and chemotherapy. *Neurology* 66(8):1258–1260
31. Moffat BA, Chenevert TL, Lawrence TS, Meyer CR, Johnson TD, Dong Q, Tsien CI, Mukherji S, Quint DJ, Gebarski SS, Robertson PL, Junck L, Rehemtulla A, Ross BD (2005) Functional diffusion map: a noninvasive MRI biomarker for early stratification of clinical brain tumor response. *Proc Natl Acad Sci* 102(15):5524–5529
32. Hamstra DA, Galbán CJ, Meyer CR, Johnson TD, Sundgren PC, Tsien CI, Lawrence TS, Junck L, Ross DJ, Rehemtulla A, Ross BD, Chenevert TL (2008) Functional diffusion map as an early imaging biomarker for high-grade glioma: correlation with conventional radiologic response and overall survival. *J Clin Oncol* 26(10):3387–3394
33. Ellingson BM, Malkin MG, Rand SD, Connelly JM, Quinsey C, LaViolette PS, Bedekar DP, Schmainda KM (2010) Validation of functional diffusion maps (fDMs) as a biomarker for human glioma cellularity. *J Magn Reson Imaging* 31(3):538–548
34. Galbán CJ, Chenevert TL, Meyer CR, Tsien C, Lawrence TS, Hamstra DA, Junck L, Sundgren PC, Johnson TD, Ross DJ, Rehemtulla A, Ross BD (2009) The parametric response map is an imaging biomarker for early cancer treatment outcome. *Nat Med* 15(5):572–576
35. Di Perri C, Battaglini M, Stromillo ML, Bartolozzi ML, Guidi L, Federico A, SDe Stefano N (2008) Voxel-based assessment of differences in damage and distribution of white matter lesions between patients with primary progressive and relapsing-remitting multiple sclerosis. *Arch Neurol* 65(2):236–243
36. Chen W, Delaloye S, Silverman DH, Geist C, Czernin J, Sayre J, Satyamurthy N, Pope W, Lai A, Phelps ME, Cloughesy T (2007) Predicting treatment response of malignant gliomas to bevacizumab and irinotecan by imaging proliferation with [18F] fluorothymidine positron emission tomography: a pilot study. *J Clin Oncol* 25(30):4714–4721
37. Sorensen AG, Batchelor TT, Zhang WT, Chen PJ, Yeo P, Wang M, Jennings D, Wen PY, Lahdenranta J, Ancukiewicz M, di Tomaso E, Duda DG, Jain RK (2009) A “vascular normalization index” as potential mechanistic biomarker to predict survival after a single dose of cediranib in recurrent glioblastoma patients. *Cancer Res* 69(13):5296–5300
38. Pope WB, Kim HJ, Huo J, Alger J, Brown MS, Gjertson D, Sai V, Young JR, Tekchandani L, Cloughesy TF, Mischel PS, Lai A, Nghiemphu PL, Rahmanuddin S, Goldin J (2009) Recurrent glioblastoma multiforme: ADC histogram analysis predicts response to bevacizumab treatment. *Radiology* 252(1):182–189
39. Ellingson BM, Malkin MG, Rand SD, Hoyt A, Connelly J, Bedekar DP, Kurpad SN, Schmainda KM (2009) Comparison of cytotoxic and anti-angiogenic treatment responses using functional diffusion maps in FLAIR abnormal regions. *Proc Int Soc Mag Reson Med* 17:1010
40. Ellingson BM, Malkin MG, Rand SD, LaViolette PS, Connelly JM, Mueller WM, Schmainda KM (2011) Volumetric analysis of functional diffusion maps (fDMs) is a predictive imaging biomarker for cytotoxic and anti-angiogenic treatments in malignant gliomas. *J Neurooncol* 102:95–103
41. Georgiades CS, Itoh R, Golay X, van Zijl PC, Melhem ER (2001) MR imaging of the human brain at 1.5 T: regional variations in transverse relaxation rates in the cerebral cortex. *AJNR Am J Neuroradiol* 22(9):1732–1737